

EVALUATION OF LLRF STABILITIES AT STF

T. Miura[#], S. Michizono, T. Matsumoto, H. Katagiri, Y. Yano, S. Fukuda, KEK, Tsukuba, Japan
 Y. Okada, NETS, Fuchu-shi, Japan

Abstract

In STF phase-1, four-cavities are operated with vector-sum feedback (FB) control. The FB control instabilities arising from passband of TM_{010} mode other than π mode were measured. Further, a feedforward (FF) table was used in combination with FB control, which improved the flatness of the flat-top region. A method for reduction of overshoot in FB + FF operation is also proposed. By electrically developing a quasi-beam, the response for quasi-beam injection was also measured, and the correction on beam-loading was performed.

INTRODUCTION

The Superconducting RF Test Facility (STF) is the R&D facility of the International Linear Collider (ILC). In the STF phase-1, four nine-cell cavities [1] were installed in a cryomodule and operated using the vector-sum feedback (FB) control [2]. They were driven by a pulse with a width of 1.5 ms and a repetition rate of 5 Hz. The rf stability of 0.07% in amplitude and 0.24° in phase is required at the flat-top region for ILC.

In this paper, we report the measurement of rf instability arising from other passband like a $8/9\pi$ mode, FB operation in combination with feedforward (FF) table improved overshoot at the leading-edge of the flat-top region, and the test on the operation using an electrical quasi-beam.

FEEDBACK INSTABILITY DUE TO PASSBAND OF TM_{010} MODE

The cavity is operated in the π mode, which has the highest efficiency for beam acceleration. In the operation with FB control, rf instability can occur due to the passband of TM_{010} mode except for the π mode [3,4]. Table 1 shows the frequency difference between the π mode and the other modes measured at each cavity at the STF. For a given mode, the frequency is different for different cavities due to fabrication error.

Table 1: Frequency differences between π mode and the other mode for each cavity.

mode	Cavity 1 $f_{\pi} - f$ (MHz)	Cavity 2 $f_{\pi} - f$ (MHz)	Cavity 3 $f_{\pi} - f$ (MHz)	Cavity 4 $f_{\pi} - f$ (MHz)
$8/9\pi$	1.1675	0.7223	1.1225	0.8859
$7/9\pi$	3.6413	3.5392	3.4742	3.3931
$6/9\pi$	6.9246	7.3201	7.0056	7.0822
$5/9\pi$	11.8131	11.6902	11.6116	11.5009
$4/9\pi$	16.0743	16.4536	16.3576	16.2954
$3/9\pi$	20.8873	20.7968	20.9104	20.6134
$2/9\pi$	24.1013	24.5003	24.4863	24.1717
$1/9\pi$	26.4603	27.2074	26.6434	26.6119

[#]takako.miura@kek.jp

Figure 1 shows the diagram of the LLRF control system [5] at the STF. The pick-up signal from each cavity is down-converted to an intermediate frequency (IF) of 10 MHz. These IF signals are sampled by 16-bit ADC at 40 MHz. Separation of I/Q components, vector-sum and FB calculations are performed on a field programmable gate array (FPGA). The baseband I/Q signals are output from a 14-bit DAC. They are fed into the IQ modulator via a 0.4-MHz low-pass filter (LPF) in order to reject the signals corresponding to modes other than the π mode.

In this study, the LPF was removed to measure the raw intensities of the signals of the other modes. A digital delay system with a clock of 40 MHz was implemented in the FPGA to observe the relation between feedback loop delay and the rf instability. The digital delay was varied between 1 and 120 clocks (3 μ s).

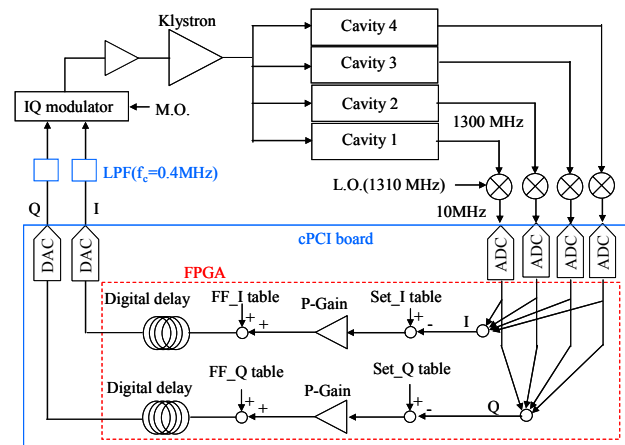


Figure 1: Schematic diagram of LLRF system. In the instability measurement arising from the other mode π mode, low pass filter placed between DAC and IQ modulator was removed.

The feedback became stable or unstable depending on the digital delay. In the case of unstable, $8/9\pi$, $7/9\pi$ and $6/9\pi$ modes are observed other than π modes in the frequency spectra. The rms values of amplitude indicating instability for additional loop delay is shown in Fig.2; the upper four graphs in the figure show the result of the FB at each cavity, while the lowest graph shows the result of the vector-sum FB operation. In the case of high gain, i.e., $p=55$, stable region is extremely narrow in individual operation because of the large excitation by the $8/9\pi$ and $7/9\pi$ modes; the position of stable region is different for each cavity, since frequencies of the $8/9\pi$ and $7/9\pi$ modes are different for each cavity. The result of vector-sum operation, therefore,

became unstable over all regions of loop delay. In the case of low gain, i.e., $p=5$, the stable region became wider. In the vector-sum operation, since the intensities of the signals from each cavity become $\sim 1/4$, less instability is observed over almost the entire range of additional loop delay.

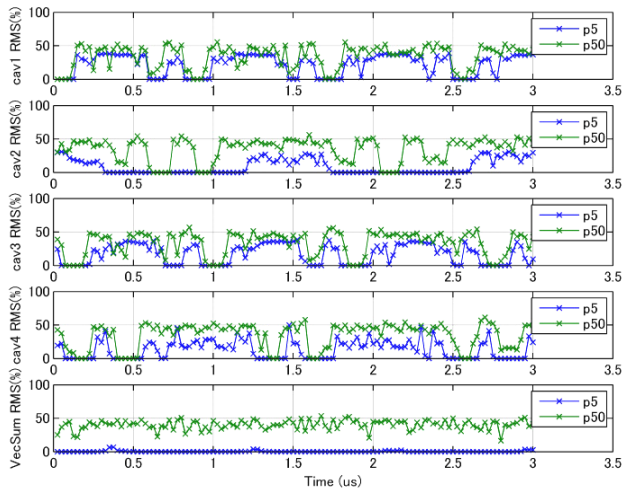


Figure 2: Result of rms values of amplitude indicating instability for additional loop delay. The upper four graphs are results of FB operation of the individual cavity, the lowest graph is the result the vector-sum operation.

FEEDFORWARD TABLE

In this section, we discuss the FB operation with the use of a FF table. The amplitude and phase of the flat-top region was measured under three operational conditions; FB, FB + FFDAC, and FB + FFSM; the measurement results are shown in Fig.4. The result under FB differs slightly from the set value, and the amplitude and phase are sensitive to the FB Gain. In contrast, in the case of the use of a FF table such as FFDAC or FFSM (see. Fig.3) in combination with FB, the results are in good agreement with the set value. The flatness observed at 700~1600 μs corresponds to 0.02% rms and 0.016° rms in the case of FB operation and 0.007% rms and 0.015° rms in the case of FB operation with a FF table. Figure 3 shows a comparison between the FFDAC and FFSM. FFDAC is the FF table whose output is the same as that from DAC in the FB operation. DAC output is used as the FF table to correct the nonlinearity of a klystron or the RF amplifier. Under FB + FFDAC condition, however, a large overshoot of 1% was observed at the leading-edge of the flat-top region. The overshoot is thought to be caused by the delay in the feedback. To compensate the delay, FFDAC should be shifted temporally forward the length of delay. FFSM is made by applying the smoothing procedure from each channel to the next X channel which is corresponding the twice the amount of the delay. The amount of delay for FB gain = 90 was approximately 20 μs for Q_L (loaded Q) = 3×10^6 and $\sim 8 \mu\text{s}$ for $Q_L = 1.2 \times 10^6$. These delay length are longer than the loop delay of the FB-circuit itself, which

is estimated to be approximately 3.26 μs (LPF: 1.476 μs + Amp: 0.763 μs + klystron: 0.123 μs + FPGA: 0.4 μs + cable/waveguide: 0.5 μs). The FB delay depends not only on QL but also on the FB gain. Under FB + FFSM condition, the overshoot decreased to 0.1% and 0.1° .

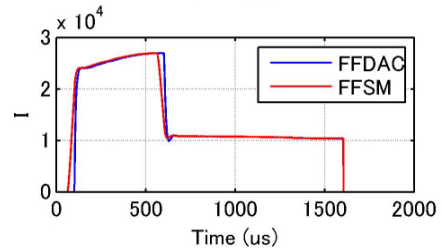


Figure 3: Comparison of FFDAC with FFSM

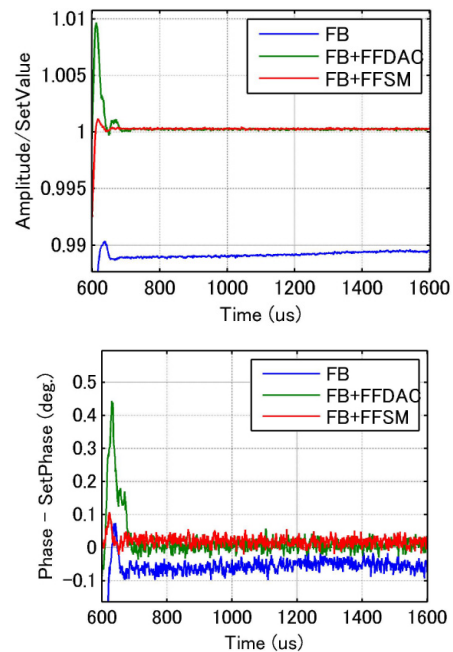


Figure 4: Comparison of amplitude and phase measured at flat-top region. Under FB + FFDAC or FB + FFSM condition, stability at 700~1600 μs is 0.007% rms and 0.015° rms.

OPERATION WITH QUASI-BEAM

In STF phase-1, the beam is not available. Therefore, to measure the response of a beam, a quasi-beam was electrically fabricated. For this, a square wave with an angle of -180° was introduced for klystron input, as shown in Fig.5. The DAC outputs of the FB operation with and without the quasi-beam are shown in Fig.6. The amplitude of quasi-beam was adjusted such that the resultant DAC outputs in FB operation had the same amplitude between the filling time (100~600 μs) and the beam injection time (812~1322 μs).

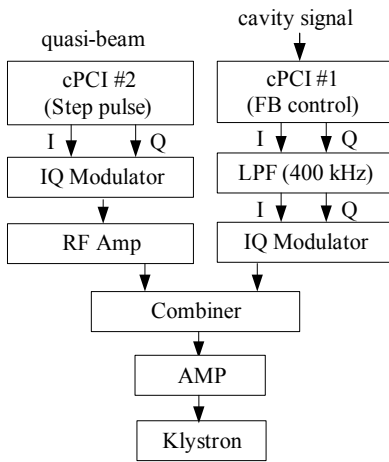


Figure 5: Block diagram of quasi-beam introduction.

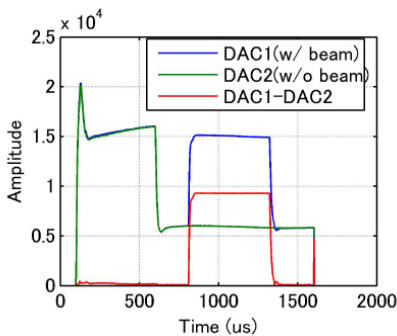


Figure 6: DAC output in FB operation with and without quasi-beam (DAC1 and DAC2, respectively) and that by subtracting (DAC1 – DAC2) that is used for FF(beam).

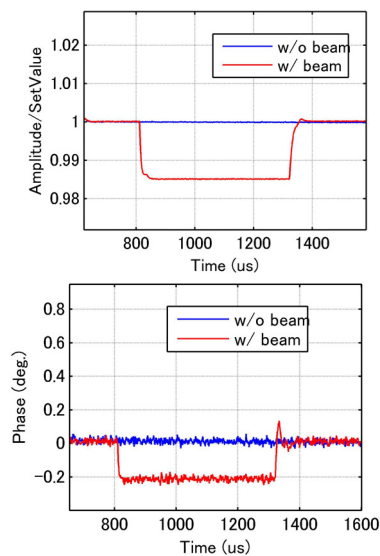


Figure 7: Difference between normal FB operation with and without quasi-beam at the flat-top. A drop of 1.5% in amplitude and 0.2° in phase by the introduction of quasi-beam was observed.

Figure 7 shows the comparison of the response of FB operation with and without the quasi-beam at the flat-top region. The quasi-beam showed a drop of 1.5% in amplitude and offset of 0.2° in phase. Therefore, beam correction using FF(beam) table was achieved by subtracting the DAC output obtained with the quasi-beam from that without it, as shown in Fig.6.

Figure 8 shows the result of measurements around the quasi-beam injection in FB + FFSM + FF(beam) operation. The timing of the FF(beam) is adjusted to minimize the overshoot or undershoot. The flatness at beam region excluding the head and tail corresponds to 0.04% rms in amplitude and 0.02° rms in phase.

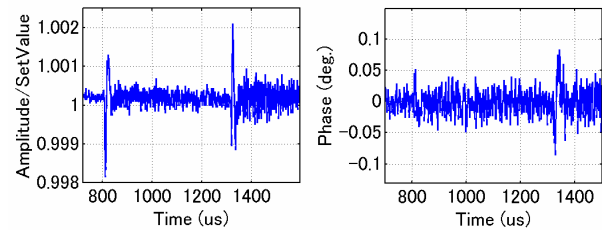


Figure 8: Flat-top stability around quasi-beam injection in FB + FF table (including beam compensation) operation with timing adjustment.

SUMMARY

The vector-sum operation for four cavities was performed at the STF. The instability arising from the other mode except for the π mode was measured. In high FB gain, the vector-sum operation become unstable over all regions of additional loop-delay. In contrast, in low FB gain, the vector-sum operation is stable over almost the entire range. In the operation of FB + FF table, 0.007% rms and 0.015° rms was achieved. Finally, tests were performed using a quasi-beam, and a FF(beam) was developed as a FF table to compensate the beam loading. By adjusting the timing of the FF(beam), the stability at beam region excluding the head and tail was achieved to be within the range required by ILC.

REFERENCES

- [1] E. Kako et al., “Cryomodule Tests of Four Tesla-like Cavities in the STF Phase-1.0 for ILC”, PAC09,(2009), TU3RAI04, in these proceedings.
- [2] S. Michizono et al., “Vector-Sum Control of Superconducting rf Cavities at STF”, PAC09, (2009) WE5FP083, in these proceedings.
- [3] E. Vogel, “High gain proportional rf control stability at TESLA cavities”, Phys. Rev. ST Accel. Beams 10, 052001 (2007).
- [4] T. Miura et al., “Measurements of Feedback Instability due to $8/9\pi$ and $7/9\pi$ modes at KEK-STF”, Linac08, (2008), THP109.
- [5] T. Matsumoto et al., “Low-Level RF System for STF”, LINAC06, (2006), THP010.